Journal of Membrane Science 697 (2024) 122564

Contents lists available at ScienceDirect

Journal of Membrane Science

journal homepage: www.elsevier.com/locate/memsci

Study on ammonia transport and separation in Aquivion® perfluoro sulfonated acid membranes

Virginia Signorini [a], Aysegul Askin [b], Claudio Oldani [c], Matteo Minelli [a], Marco Giacinti Baschetti [a,*]

[a] Department of Civil, Chemical, Environmental and Materials Engineering, University of Bologna, Via Terracini 28, Bologna, Italy
[b] Department of Chemical Engineering, Faculty of Engineering and Architectural, Eskisehir Osmangazi University, 26040, Eskişehir, Turkey
[c] Solvay Specialty Polymers Italy S.p.A., Viale Lombardia 20, 20021, Bollate, MI, Italy

ARTICLE INFO

Keywords:
Ammonia
Aquivion
Gas separation
Gas sorption
Gas diffusion

ABSTRACT

The present study reports the results of a series of sorption and permeation tests of pure ammonia as well as nitrogen and hydrogen carried out on Aquivion C87-05 (short-side chain perfluoro sulfonic acid ionomer). Such material is indeed of interest for possible applications in sustainable processes for ammonia production, either as base material for polymer electrolyte membranes in low-temperature electrochemical ammonia synthesis or as a membrane for effective product separation.

NH_3, N_2, and H_2 permeation tests are performed at different temperatures (20, 35, and 50 °C) and both in dry and humid conditions (R.H. up to 80%), aiming to assess the influence of these parameters on the resulting permeabilities, while ammonia sorption is inspected at the same temperatures, and pressures up to near saturation conditions.

Pure ammonia permeability reached outstanding values around 7000 Barrer in dry Aquivion membranes, revealing an increasing trend with upstream pressure, while it decreased with temperature. The same behavior is recorded for NH_3 solubility, indicating that sorption drives the ammonia transport through the membrane.

The obtained separation performances are found to be significantly better than those of other polymeric membranes proposed for the same separations, as compared to a permeability-selectivity plot.

1. Introduction

Ammonia is one of the most important compounds in the chemical industry and it is a key chemical component for various relevant applications such as pharmaceutical and chemical processes, production of fertilizers, and refrigeration systems just to mention some [1–3]. Furthermore, over the last few years, NH_3 is attracting new interest as an energy carrier, as it may be used in combustion engines or high-temperature electrochemical systems, due to its appealing thermal and physical properties [2,4–6]. Besides, NH_3 is also a suitable candidate for hydrogen (H_2) storage and transport, thanks to its high storage density and lower energy demand for liquefaction (NH_3 may be readily liquefied at −33 °C at 1 bar) [6]. In the strategy for the implementation of a hydrogen economy and the mitigation of global warming, therefore, NH_3 represents an ideal carbon-free energy carrier, combining low emissions with efficient long-distance transportation [3,7].

However, the state-of-the-art ammonia synthesis process is still based on the Haber-Bosch method [8,9], which is not environmentally friendly. The endothermic reaction between N_2 and H_2 needs to be carried out at high temperatures and pressure, and it requires large amounts of heat, currently obtained from fossil fuels [10,11]. Moreover, NH_3 emissions in the atmosphere can react with acid compounds to form haze secondary particles [12].

Therefore, the key challenge to develop an ammonia-based energy system is to set up a competitive process able to synthesize and purify NH_3, in a reliable and scalable way, while reducing its environmental footprint [13]. The combination of green ammonia production, efficient ammonia purification, and reutilization with clean renewable power is indeed needed to build a green ammonia energy economy [14].

Among the others, electrochemical synthesis to produce ammonia at low temperature and pressure, using renewable energy [3], has gained a lot of interest, especially when coupled to an efficient separation process. In this concern, the membrane-related process might be a really promising technology in such applications for the lower cost combined

* Corresponding author. Department of Civil, Chemical, Environmental and Materials Engineering, University of Bologna, via Terracini 28, I-40132, Bologna, Italy.
E-mail address: marco.giacinti@unibo.it (M. Giacinti Baschetti).

https://doi.org/10.1016/j.memsci.2024.122564
Received 21 December 2023; Received in revised form 5 February 2024; Accepted 9 February 2024
Available online 10 February 2024

to high purity and the possibility of a continuous process [15,16].

Pressure-driven gas separation processes by membranes are in this concern natural candidates for such application, as ammonia high condensability usually provides higher permeability with respect to lighter components, such as N_2 and H_2 [17]. Moreover, ammonia separation through highly selective membranes is a sustainable process due to the simplicity of the process and the low energy consumption [11,18,19].

The separation performances of polymeric membranes are determined by two main parameters: permeability, which describes how fast molecules are transported through the material, and selectivity, indicating the ability of the membrane to separate one component from the rest [20–22]. Such quantities, however, are limited by a typical trade-off, defined by Robeson in the late 20th century [23,24], whose upper bound represents still today a suitable tool for the evaluation of the potentiality of membrane materials for a given separation. In this context, many materials have been proposed for such separation, demonstrating a fast and highly selective permeation [10,18,25]. Inorganic (MXene [19], silica [11], zeolite [26]) and polymeric (Nafion, Aquivion [18], Cellulose [27], Polystyrene (PS) [28,29], zeolitic imidazolate frameworks (ZIF) [17], Prussian Blue [30]) membranes have been studied for ammonia separation, revealing that both large values of ammonia permeability and selectivity (with respect to N_2 and H_2), can be achieved in different operating conditions.

He and Cussler [18], as well as other authors [25,31,32], have reported the use of Nafion and other PFSA materials for NH_3 separation, both as a flat and hollow fiber membrane. The results obtained show a pronounced affinity between ammonia and the sulfonic group, thus leading to remarkably large NH_3/H_2 and NH_3/N_2 selectivities. Following such concept, the present work focuses on another sulfonic acid ionomer, the Aquivion C87-05, similar to Nafion but with a shorter pendant side chain, which is also characterized by high thermal and chemical stability [33–35].

Although, some studies dedicated to the investigation of these PFSA materials' properties are already available in the literature for what concerns ammonia permeation and transport, a complete and comprehensive characterization is lacking to date, especially about the effect of temperature, pressure, and humidity on membrane performances. Therefore, Aquivion membranes have been studied via transient sorption and steady-state permeation experiments to understand the gas transport in dry and humid polymeric matrices. The attention is devoted to pure component transport aiming to describe ammonia diffusion and permeation through the polymeric matrix [34], and at a deeper understanding of the potential of Aquivion for green ammonia synthesis and purification.

2. Materials

The material characterized in this work is Aquivion® C87-05 (Equivalent weight EW = 870 g_{pol}/mol_{SO3H}), a perfluorosulfonic acid ionomer membrane, produced by a solvent-casting process and kindly provided by Solvay Specialty Polymers Italy S.p.A. (Bollate, Milano, Italy). Aquivion C87-05 is characterized by a thickness of 50 μm and a density of 1.93 g/cm^3, while its chemical structure is displayed below in Fig. 1. Its characteristic short-side chain has been obtained by the copolymerization of Tetrafluoroethylene (TFE) and Sulfonyl Floride Vinyl Ether (SFVE), conferring to the material good thermal stability and high mechanical properties.

Due to its high hydrophilicity, which may affect materials properties, Aquivion samples have been treated overnight under vacuum at 50 °C before each test, to ensure appropriate and repeatable membrane drying.

Sorption and permeation tests are performed by using pure NH_3 (purity of 99.99%), provided by SIAD, while H_2 and N_2 (99.99% purity) are obtained from Fluido Tecnica s.a.s (Campi Bisenzio, Firenze, Italy).

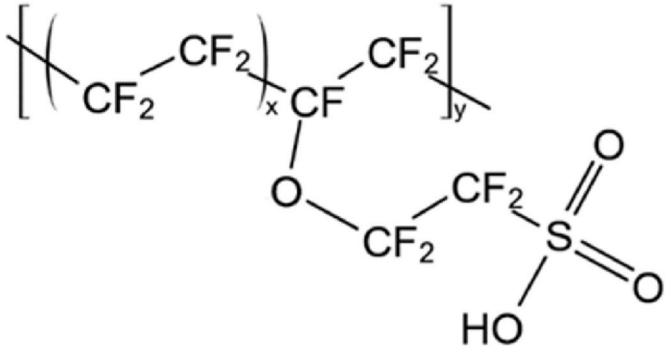

Fig. 1. Short-side chain chemical structure of Aquivion® C87-05.

3. Methods

The most important property of membranes is their ability to control the permeation rate of different species. Usually, the transport of low molecular weight gases through a dense polymeric membrane is governed by the solution-diffusion mechanism [36]. As revised by Wijmans and Baker [37], in a membrane separation process, the permeants are separated given their different solubility and rate of diffusion in the polymeric material. According to this approach, the fluid, in contact with the polymeric layer, is absorbed in the upstream side, diffuses across the matrix, and it is then desorbed in the low-pressure compartment. Diffusion usually controls the process according to Fick's law (Eq. (1)),

$$J_i = -D_i \frac{dc_i}{dx} \tag{1}$$

where J_i is the steady-state flux of the species i, D_i is the diffusion coefficient and $\frac{dc_i}{dx}$ is the concentration gradient, which acts as the driving force of the process [38]. It is then assumed that the fluid on either side of the gas/polymer interface is at equilibrium and so the chemical potential is continuous at the interface. The penetrant concentration (c_i) in the matrix is correlated to the partial pressure (p_i) in the gas phase through a solubility coefficient, S_i:

$$c_i = S_i\, p_i \tag{2}$$

The flux can be rewritten in terms of permeability coefficient P_i as follows:

$$J_i = P_i \frac{\Delta p_i}{l} \tag{3}$$

where l is the thickness of the membrane, Δp_i is the partial pressure gradient of component i. Therefore, combining Eqs. (1)–(3), the permeability P_i may be described as $P_i = S_i D_i$ [37,39].

Gas permeability describes how penetrant molecules dissolve into the membrane and migrate across the matrix. High permeability, then, can result from high solubility, high diffusivity, or a favorable combination of the two, depending on the polymer nature, structure, and chemical behavior, as well as on the properties of the penetrants. In addition to that, it is noteworthy to mention that, permeability also influences separation efficiency, because the selectivity of the membrane ($\alpha_{i,j}$) in ideal conditions is equal to the ratio between the most (P_i) and the less (P_j) permeable fluids in the material, as shown in Eq. (4):

$$\alpha_{i,j} = \frac{P_i}{P_j} = \frac{S_i}{S_j} \bullet \frac{D_i}{D_j} \tag{4}$$

In general, permeability, diffusivity, and selectivity allow to completely characterize the mass transport properties of a given gas-polymer pairs and can be determined experimentally by means of direct permeation and transient-sorption measurements.

In this work, the system used for the experimental characterization of Aquivion membranes is reported in Fig. 2. The custom-made apparatus, which is immersed in a thermostatic bath to ensure temperature control, can carry out both permeation and sorption tests. In this apparatus, the pressure variation is registered by a Honeywell pressure transducer PT03 (0–500 psia), while the temperature is maintained constant thanks to a Julabo – Corio C thermostat.

3.1. Pure sorption experiments

The solubility and diffusion coefficients of NH_3 in Aquivion membrane have been measured by transient-sorption experiments in the above-mentioned apparatus with a pressure decay configuration obtained by closing valve V12, shown in Fig. 2. Such configuration allows the determination of the amount of gas sorbed into a certain volume of materials by measuring the pressure change in a closed calibrated volume. Briefly, a known quantity of polymers is inserted into a sample chamber (volume V_C connected through valve V5), while the penetrant gas is loaded in the pre-chamber (volume V_P connected to valve V6) at the desired pressure. The NH_3 mass uptake in the polymer is determined by measuring the pressure decrease over time once the pre-chamber and the chamber are connected, until reaching the equilibrium pressure. The measured pressure drop can be indeed related to the moles absorbed through Peng-Robinson (PR) equation of state, since both values of temperature and volume of the systems are known. Subsequently, sorption tests are performed by increasing the loading pressure in a stepwise manner, to obtain the sorption isotherm in the pressure range of interest. The complete procedure of the pressure decay technique is better explained in a previous publication [40].

The technique allows also to evaluate the diffusion coefficient D in the dense polymeric layer by considering the pressure evolution with time, using the suitable solution of Fick's law provided by Crank [41]:

$$\frac{n_t - n_0}{n_\infty - n_0} = 1 - \sum_{i=1}^{\infty} \frac{2\alpha(1+\alpha)}{1+\alpha+\alpha^2 q_i^2} \exp\left(-\frac{4Dq_i^2 t}{l^2}\right) \quad (5)$$

Where n_t is the number of molecules of NH_3 dissolved in the polymer sample at time t, while n_∞ and n_0 are the number of moles present at the infinite time and at time equal to zero, respectively. Moreover, l is the thickness of the sheet, q_n is the non-zero positive roots of the equation $\tan(q_n) = -\alpha q_n$ with $\alpha = 2KV_{tot}/l$, being K the penetrant partition coefficient between the gas and the polymeric phase.

3.2. Pure permeation experiments

Permeation experiments are carried out in the same experimental system described above, using a constant volume and variable pressure permeation method. In this concern, the Aquivion membrane is located into the sample holder, which presents an effective membrane area of 9.62 cm^2, in direct contact with an agitated reservoir, while valve V12 is open allowing the permeant flow from the cell to the calibrated downstream volume (Fig. 2).

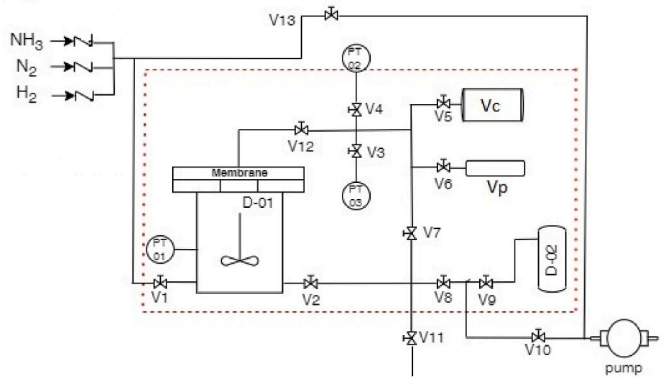

Fig. 2. Pure and mixed permeation and pressure decay apparatus scheme. The dotted line represents the surface of thermostatic bath control.

In the pure dry gas tests, the measurements start when the NH_3 is fed into the upstream tank, while the downstream volumes are kept under vacuum, thus creating the pressure gradient that represents the driving force of the process. The gas flux across the membrane, and thus the permeability, is calculated through the registration of the pressure increase over time in the calibrated downstream volume. In case of humid tests, a preliminary equilibration step is required to saturate the membrane at the desired water activity before the permeating gas (at the same R.H.) is fed [42].

In both dry and humid conditions, permeability of the penetrant i, P_i at steady state is calculated, through Eq. (6), where ideal gas assumption is considered since the compressibility factor, that accounts for the deviation from the ideality, is almost 1 in the downstream pressure range inspected for this work:

$$P_i = \left.\frac{dp}{dt}\right|_{s.s.} \frac{V_d}{RTA} \frac{l}{(p_i^{up} - p_i^{down})} \quad (6)$$

where $\left.\frac{dp}{dt}\right|_{s.s.}$ is the steady state pressure change in time of downstream compartment, V_d is the downstream volume, A the membrane surface area, T the fixed temperature of the system, R is the universal gas constant, (p_i^{up}-p_i^{down}) is the partial pressure difference of component i across the membrane and l the membrane thickness, which is considered constant during the calculation, thus neglecting the swelling of the membrane upon ammonia sorption.

From the permeation experiments, one can determine not only the gas permeability, but also the diffusion coefficient, using to the so-called time-lag method, which measures the time difference observed between the beginning of the test when the penetrant enters the membrane and the time at which the flow rate of diffusing species into the closed volume reaches a steady state [43,44]. The time lag θ is determined as the time-axis intercept of the linear portion of the downstream pressure curve, as this quantity can be related to diffusion coefficient through Eq. (7) [43,45]:

$$\theta = \frac{l^2}{6D} \quad (7)$$

3.3. FT-IR

The FTIR analysis has been used in this study to inspect the presence of any residual NH_3 in the polymeric matrix after sorption/permeation measurements and to evaluate any possible alteration of the polymer membrane upon exposure to ammonia. FTIR-ATR (Fourier transform infrared-attenuated total reflectance) spectroscopy, indeed, is capable of labeling molecules and functional groups based on their interaction bonds with the polymer atoms and following their evolution with time and penetrant activity [46,47]. The measurements are conducted with a Nicolet Avatar 6700 FTIR, equipped with a liquid nitrogen-cooled mercury−cadmium−telluride detector and a single bounce zinc selenide ATR crystal (Pike Miracle Technology) with an incident angle of 45°. The data are collected by subtracting the air background and averaging 128 scans per spectrum with a resolution of 4 cm^{-1}.

At each infrared scan, the radiation wave rises from the surface, and it is then reflected onto the crystal and absorbed by the polymer interface, eventually leaving the opposite face of the ATR element for the detection of the spectrum [48,49].

4. Results and discussion

4.1. FTIR

The effect of ammonia exposure on the Aquivion film has been evaluated by FT-IR, inspecting if any permanent change has been induced by the material. Fig. 3 reports the FT-IR spectra obtained for pristine Aquivion C87-05 (black line), and after the exposure at 35 °C to NH_3 up to 7 bar, and water vapor only (green and red lines respectively), together with the Aquivion spectrum after 30 days from NH_3 treatment. As one can see, both H_2O and NH_3 produce a significant effect to the chemical footprint of the polymer, and new characteristic peaks appear in the spectrum range investigated.

In detail, the main absorption bands that characterize Aquivion are located in the wavenumber interval between 900 and 1300 cm^{-1}. In particular, the two highest peaks, around 1155 and 1220 cm^{-1}, are usually ascribed to symmetric and asymmetric –CF bonds, respectively, while COC bond is detected at 970 cm^{-1}. The sulfonated acid stretching arises at 910 cm^{-1} for the undissociated S–OH bond, while the bands related to the S═O group do not appear at 1410 cm^{-1} as expected, probably because such moiety is already dissociated due to ambient air humidity [51–54]. Moreover, the peak related to the symmetric $–SO_3^-$ dissociated ion is located approximately at 1057 cm^{-1} [52,53], while around 1300 cm^{-1} all the spectra show a shoulder-like behavior associated to the asymmetric peak of $–SO_3^-$; such peak becomes more pronounced upon exposure to ammonia, revealing the proton transfer reaction that occurs due to the possible formation of clusters [51–54]. The presence of ammonia characteristic groups is indicated by the NH stretching in asymmetrical bending mode in the region between 1500 and 1700 cm^{-1}, while symmetrical bending is around 850 and 980 cm^{-1} [46,55].

The characteristic peaks associated to the presence of water molecules are clearly visible in the spectrum of Aquivion specimen after exposure to water at 80% R.H. (red line): at 1500-1700 cm^{-1} for H–O–H bending and in the wavenumber range between 2500 and 3800, related to the vibration of –OH groups, which exhibit a maximum around 2800 cm^{-1} [50,56]. The behavior of this large band is not univocally identified due to the overtone of bending modes, but the most feasible explanation is related to the swelling of the membrane upon hydration [53]. Although much less obvious, those peaks can be detected also in the NH_3-treated spectrum, thus confirming the swelling hypothesis.

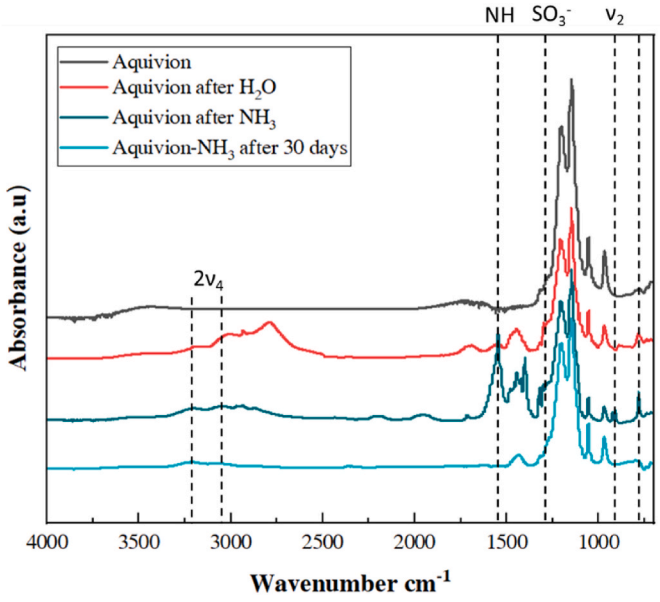

Fig. 3. *FTIR-ATR absorption spectra of pristine Aquivion C87-05 (black), after its exposure to H_2O vapor(red) and NH_3 gas (green). The cyan line represents the spectra of Aquivion treated in NH_3 after 30 days in atmospheric conditions (shifted for clarity shake)* [50]. (For interpretation of the references to colour in this figure legend, the reader is referred to the Web version of this article.)

Interestingly, as reported in previous works available in the technical literature [55,56], the IR characteristic band located in the range from 1300 to 1500 cm^{-1} is associated to the ammonium ion or amide group, suggesting the formation of some chemical bonds between NH_3 and Aquivion surface sites, even if the material structure does not change irreversibly [31]. The spectrum recorded right after ammonia tests (green line) displays different vibrational stretching mode between 2750 and 3300 cm^{-1}. It has been reported [57–61] that ammonia small clusters exhibit a FTIR response characterized by four vibrational modes, two of which are clearly visible in Fig. 3 for Aquivion-NH_3 complex: the degenerated overtone NH bending mode $2\nu_4$ appears between 3200 and 3250 cm^{-1}, while ν_2 represent the umbrella mode bands that arise around 978/983 cm^{-1}.

Finally, the analysis of Aquivion spectra after its exposure to ammonia gas reveals that ammonium ions remain bonded to the polymer chains after absorption. It is interesting to notice, however, that the chemical bonding between ammonia and a sulfonic group in the membrane seems reversible: indeed, the FTIR spectrum of the "NH_3-treated" Aquivion sample (cyan line in Fig. 3) returns almost equal to those of the pristine material after about 30 days in atmospheric conditions, meaning the ammonia release is basically complete even though very slow if compared to the sorption process, as will be better shown in the following.

4.2. NH_3 transient sorption experiments

The measured ammonia solubility in Aquivion at 20, 35 and 50 °C is illustrated in Fig. 4 in terms of λ, that is the number of moles of NH_3 absorbed per mole of $–SO_3H$ in the membranes, plotted with respect to penetrant activity (the ratio between experimental pressure P and ammonia vapor pressure P* [62]). Since, to the best of our knowledge, no similar data are present in the literature for this type of material, the results have been compared with those of water vapor in PerFluoroSulfonated Ionomer (PFSI) membranes (equivalent molecular weight of 860 g_{pol}/mol_{SO3H}) [63]. Interestingly, the measured ammonia uptake is significantly larger than that of water at all temperatures, thus confirming the material strong affinity to the vapors of alkaline substances [45–47]. As one can see, the NH_3 solubility isotherms show a sharp and concave increase with activity followed by a more linear behavior, which seems to terminate with a concavity change for activities larger than 50%. Such change in concavity, however, is apparent at 20 °C, but only barely visible at higher temperatures. The same behavior has been observed also for water solubility in PFSI, even if much weaker. That has to be ascribed to the strong interaction of the polar penetrants (either H_2O or NH_3) with the SO_3H group that leads at low activity to a sort of adsorption-like behavior, while at high activity it causes swelling of the matrix and leads to the formation of a phase segregated structure, where sulfonated (hydrophilic) domains are interpenetrated with fluorinated hydrophobic sections [35,64–66].

Sorption kinetics are in good agreement with Fickian diffusion behavior, even in the case it is accompanied by an instantaneous reaction, as reported by Crank [41], that is when the absorption process can be considered linear. Therefore, the diffusion coefficient of NH_3, displayed in Fig. 4b as a function of average penetrant content in each sorption step has been evaluated from the transient mass uptake curve by using Eq. (5). The experimental sorption tests, indeed, always showed good agreement with Eq. (5) prediction in line with what observed for example for water in the same materials [67–69].

As often observed, the diffusion coefficient increases with the penetrant concentration and temperature. The diffusivity values lay between 10^{-8} and 10^{-7} cm^2/s, in line with the results obtained by Timashev et al. for ammonia diffusion in perfluorinated hollow fibers [31].

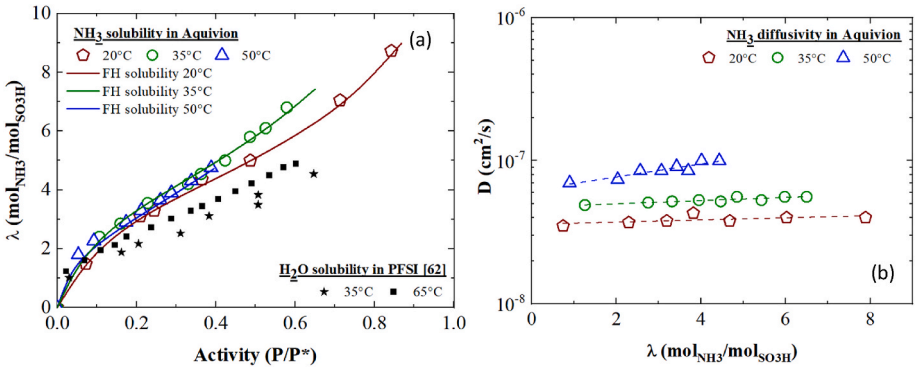

Fig. 4. *(a) Comparison between NH_3 and H_2O vapor uptake versus activity* [62]*, coupled with Flory-Huggins modeling (curves), (b) NH_3 Diffusion coefficient at 20, 35 and 50°C.*

If compared with water diffusion in similar perfluorosulfonated materials, it can be noticed that the values of NH_3 diffusion coefficients are comparable to those of H_2O in the same range of temperatures [63,70]. However, while a clearly defined trend for H_2O diffusivity with concentration (or activity) cannot be detected, the one from NH_3 seems, instead, to be well-established and follows a purely Fickian behavior in the whole concentration range, which results in a more or less constant and monotonous diffusivity trend with concentration.

On the other hand, the data of water diffusivity in PFSA membranes reported in literature are very scattered, and they show diverse trends according to the technique used for their determination, as stated by Hallinan et al. [70] and Kusoglu et al. [64], suggesting the existence of distinct water-transport mechanisms occurring at different time- and length scales. Few studies reported a rapid increase of water diffusivity at lower penetrant concentration, until reaching a maximum value, followed by a slow decrease at increasing activity [63,71,72]. Conversely, Zelsmann et al. [69] described a linear trend of water diffusion coefficient with concentration, more similar to the one observed in this work, in which a weak behavior of NH_3 kinetic mobility in Aquivion with the penetrant uptake or its activity, is observed [57–62]. As already discussed by Laporta et al. [52], the characteristic trend of water diffusivity has to be ascribed to the peculiar sorption behavior related to the hydration of the SO_3H groups, which dissociate in SO_3^- and H_3O^+. In a similar fashion, the molecular transport of ammonia in the Aquivion material might be dictated by the affinity between the basic penetrant and the acid functional groups of the polymer which split in SO_3^- and H^+, favoring the interaction with the NH_3 clusters and promoting their diffusion [31,73–75]. In this concern, it should be noticed that for a system where strong interaction exists between the polymer and the penetrant, Fick's law still holds providing that the interaction reaches the equilibrium instantaneously with respect to the diffusion process [41].

Given this consideration, also the solubility data can be explained, by allowing for the interaction between the penetrant gas and the polymer matrix, thus using a model similar to the one proposed by Futerko and Hsing to describe water sorption in Nafion [75]. In particular, their approach, based on a revisited Flory Huggins (FH) equation that accounts for the proton transfer between the SO_3H and water, can be adapted to NH_3, by considering the following set of (n) equilibrium reactions:

$$\text{-}SO_3H + NH_3 \rightleftarrows [\text{-}SO_3^- + H^+(NH_3)]$$

$$[\text{-}SO_3^- + H^+(NH_3)] + NH_3 \rightleftarrows [\text{-}SO_3^- + H^+(NH_3)_2]$$

$$\ldots [\text{-}SO_3^- + H^+(NH_3)_{i\text{-}1}] + NH_3 \rightleftarrows [\text{-}SO_3^- + H^+(NH_3)_i]$$

$$\ldots [\text{-}SO_3^- + H^+(NH_3)_{n\text{-}1}] + NH_3 \rightleftarrows [\text{-}SO_3^- + H^+(NH_3)_n] \quad (8)$$

which can be applied to represent ammonia solubility and proton conductivity in PFSAs, as already discussed in the literature [64,76,77].

The results obtained from the FTIR characterization (Fig. 3) provide the experimental rationale for the model, demonstrating the reaction between –SO_3H group and NH_3 from new bands that appeared in the Aquivion spectra after being exposed to the alkaline gas.

According to the FH model, the ammonia activity a is correlated to the volumetric fraction of the polymer in the mixture, φ, by equation (9):

$$a = (1-\varphi)e^{\left[\left(1-\frac{1}{r}\right)\varphi+\chi\varphi^2\right]} \quad (9)$$

Where χ is the FH polymer-solvent interaction parameter. The parameter r is defined as the molar volume ratio of the polymer with respect to that of penetrant $r = (EW/\rho_{Aq})/(MW_{NH_3}/\rho_{NH_3})$, being EW the Aquivion equivalent weight, ρ_{Aq} its density, while MW_{NH_3} is the ammonia molecular weight and ρ_{NH_3} the penetrant density in the condensed state. Assuming that ammonia and the sulfonic groups of Aquivion creates an ionic/hydrogen bonds when in contact, it is reasonable to take this proton complex-reaction into account and to rewrite the volume fraction by considering $\lambda_{c,i}$ as the fraction of –SO_3H groups converted to [-SO_3 H $(NH_3)_i$] complex for each activity step. When the reaction occurs through n consecutive additions as shown in Eq. (8), therefore, φ can be written as in the following Eq. (10), which includes the possibility to have multiple ammonia molecules bounded to the same SO_3H group that fills up as the system becomes saturated:

$$\varphi = \frac{r+\sum_1^n \lambda_{c,i}}{r+\sum_1^n \lambda_{c,i}+\lambda_{free}} = \frac{r+\sum_1^n \lambda_{c,i}}{r+\lambda} \quad (10)$$

Where λ_{free} represents the number of free (non-solvated) NH_3 molecules in the polymer, which, summed to the bonded ones, leads to the total absorbed ammonia, that is λ.

In order to determine the extent of formation of the proton-transfer complex within the membrane (according to the reaction reported in Eq. (8)) the fraction of-SO_3H groups interacting with i ammonia molecules, $\lambda_{c,i}$, can be related to the equilibrium constant K_i for each consecutive absorbates association through Eq. (11) [78], which holds true for every i, with the assumption that $\lambda_{c,0}$ referring to the initial amount of free SO_3H group in the membrane must be equal to 1:

$$K_i = \frac{\lambda_{c,i}}{(\lambda_{c,i-1}-\lambda_{c,i})\,a} \quad (11)$$

The simultaneous resolution of Eqs. 9–11 allows the determination of total water uptake, λ, once the values of χ and K_i (considering a constant energy binary interaction parameter χ with concentration), are determined. Of course, to run the analysis also the maximum number of ammonia molecules per cluster (n in Eq (8)) must be defined.

In this concern, it should be noticed that, when a single reaction is considered, the modified FH equation reported above tends to underestimate the sorption curves; therefore, the modeling approach suggests

that different ammonia molecules can interact with –SO_3H groups to form rather stable clusters, in line with previous findings [53,61,79,80]. Such hypothesis is further supported by the FTIR spectra (Fig. 3) in which NH vibrational stretching mode is observed between 3200 and 2800 cm^{-1} [57,59]. Therefore, it is supposed that stable ammonia clusters create a "shell-like structure" around sulfonic groups with an NH_4^+ ion in the center, bound to SO_3^-, surrounded by neutral, but strongly polarized, NH_3 molecules that interact with dissociated sulfonic groups or with ammonium ions through hydrogen bonds [60,81–83].

From a mathematical point of view, this approach allowed to represent the NH_3 solubility in the whole range of penetrant activity and at the three temperatures investigated, by considering the presence of tetrameric NH_3 clusters [80,84], and thus leading to a model with 5 parameters (χ and K_i with i = 1.4) for each temperature. In this concern it should be noted that the experimental solubility isotherms could also be described well considering the interaction between three ammonia molecules for each –SO_3H group; however, a tetrameric ammonia cluster is considered in this work, since the formation of the proton-transfer complex with –SO_3H group in four consecutive reactions leads to a certain ion stability. It is indeed well known that tetramers are among the most stable NH_3 clusters that could be found in solutions, because their cyclic structure helps the formation of stable H bonds [61,82,85]. Furthermore, the use of additional parameters allowed to describe the experimental data with meaningful temperature-dependent quantities (K_i and χ) that resulted to follow an exponential trend with the inverse temperature (Table 1). The obtained values of χ, controlling the solubility behavior in the final part of the curve at high activity, range from 0.68 to 1.07 and are lower than those found for water [75]; they suggest slightly unfavorable interactions between the polymer and the sorbent likely related to the resistance to swelling of the hydrophobic crystalline domains of the polymer. The K_i parameters describe the downward concavity of the uptake curves; the obtained values are quite large (up to 60), confirming the strength of the interaction accounted, and generally show a decreasing behavior with the distance to the sulfonic groups (1 is the nearest, 4 the more distant), in agreement with the expectation that weaker interaction should be found for the outer shells of the cluster [86].

The ammonia solubility in Aquivion exhibits a weak temperature dependence (Fig. 4a) due to the small positive mixing enthalpy of the penetrant-matrix couple ΔH_{mix}, as determined by Van't Hoff equation, in line with what has already been reported in previous works [63,73,75]. The activation energy of sorption ΔH_S could also be determined considering the contribution of the partial molar enthalpy of mixing ΔH_{mix}, accounting for polymer/penetrant interaction, and the heat of condensation ΔH_c:

$$\Delta H_{mix} = \Delta H_S - \Delta H_C = R\left(\frac{\partial \ln a}{\partial\left(\frac{1}{T}\right)}\right)_{\lambda} \tag{12}$$

where λ is the NH_3 uptake, a is the activity, R is the ideal gas constant and T is the temperature. The obtained values of the enthalpy of mixing span from 10.1 to 2.2 kJ/mol (in the range $\lambda = 0 \div 4.5$ mol_{NH3}/mol_{SO3H}).

As far as diffusivity is concerned, its thermal behavior shows an increasing D trend with T, with an activation energy E_D for NH_3 in Aquivion that can be calculated by the Arrhenius law (Eq. (13)), ranging from 18.6 to 23.8 kJ/mol ($\lambda = 0 \div 4.5$ mol_{NH3}/mol_{SO3H}):

Table 1
Flory-Huggins parameters.

	χ	K_1	K_2	K_3	K_4
20 °C	1.07	20	20	20	20
35 °C	0.75	30	25	10	10
50 °C	0.68	60	30	5	5

$$E_D = -R\left(\frac{\partial D}{\partial\left(\frac{1}{T}\right)}\right)_{\lambda} \tag{13}$$

4.3. Permeability results

The results of permeation experiments of ammonia in Aquivion are reported in Fig. 5 as a function of upstream ammonia activity at the three temperatures investigated (20, 35, and 50 °C). Moreover, in the same figure, the permeability calculated from D and S is also reported, as obtained from transient sorption experiments by considering the solution-diffusion transport mechanism ($P = S{\cdot}D$).

As one can see, NH_3 permeability in Aquivion exceeds 17000 Barrer at 20 °C, and it decreases with temperature (8000 Barrer at 50 °C) following a concave behavior with upstream activity.

The comparison of the permeability from direct permeation and $S{\cdot}D$ from transient-sorption demonstrates that the ammonia permeation does not follow solution-diffusion transport: the values of P are at least one order of magnitude larger than $S{\cdot}D$. It is also interesting to notice that the permeability trends observed show the opposite concavity with respect to the NH_3 activity within the two methods. Such behavior can be explained by considering that Aquivion is a non-homogenous material, in which diffusion results to be significantly faster in the ionic domains rather than in the fluorinated phase. The same feature, indeed, was proven to happen for water [64,68,73,87,88], where the diffusivity determined from steady-state and transient sorption experiments do not match in the case of complex materials, such as Nafion or other perfluorosulfonated membranes

Furthermore, the endothermic temperature behavior of permeability (with E_P values ranging from −9 to −5 kJ/mol) shows an opposite trend with respect to $S{\cdot}D$, as readily obtained from $E_P = E_D + \Delta H_S$, that provides a positive activation energy around 5 kJ/mol. Such results proves that the transport of ammonia in Aquivion cannot be described as a simple solution-diffusion mechanism, because a complex interaction occurs between the alkaline ion and sulfonic groups.

To better understand the situation, a direct determination of diffusion coefficient has been carried out also during the permeation tests, by the time-lag method; the results obtained are displayed in Fig. 6. Please note that the measured NH_3 time lag is quite short, in the order of 40 s and may be affected, more than the sorption tests, by the presence of

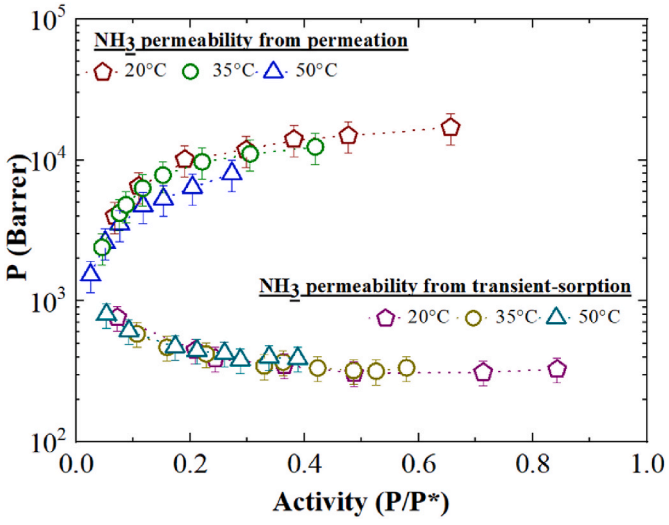

Fig. 5. Comparison between pure NH_3 permeability in Aquivion at three temperatures: 20, 35, and 50 °C, obtained from direct permeation experiments, and NH_3 permeability obtained from transient-sorption experiment (P = DS) as a function of upstream ammonia activity.

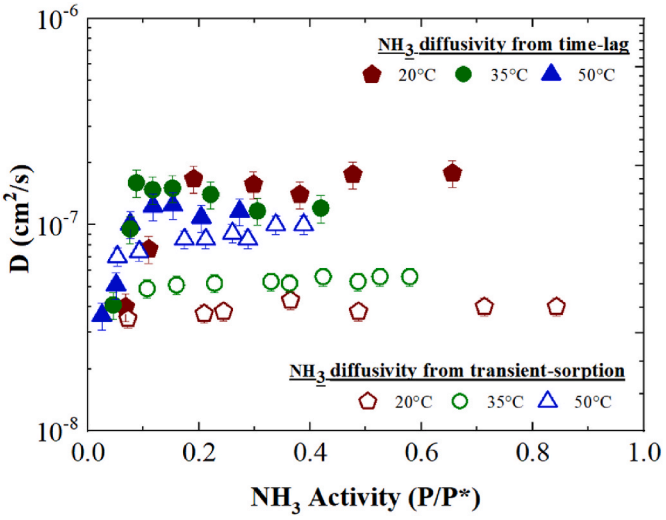

Fig. 6. Comparison between diffusion coefficients obtained permeability by applying the time-lag method and from transient-sorption experiment as a function of average activity.

solvated ammonia molecules which indeed delay the transition of ammonia in the polymer especially at low activity thus increasing the uncertainty of the obtained values. Despite this situation, the permeation-based diffusivities have an order of magnitude comparable to those obtained from transient sorption, even if they show a substantially different trend. The diffusion coefficients calculated through the time-lag method seem to decrease with temperature and show a sharp increase for activity values lower than 0.2, followed by a constant value at higher activities. Such behavior as said above is likely related to the formation of solvated ammonia ion domains that, at low activity slow down the initial ammonia transport while, at higher activity, become interconnected, thus providing a preferential pathway for penetrant transport, and leading to an appreciable increase of the apparent diffusivity. In this concern, it is worthwhile to mention that also sorption and permeation isotherms show a change of concavity approximately in the same activity range, which may suggest that the evolution of the transport process inside the materials is also related to the substantial completion of the ammonia cluster formation (or at least of its inner shells) around the sulfonic groups.

Fig. 6, together with Fig. 5, indicates that the main contribution to ammonia transport is given by solubility, being the diffusion coefficient from transient sorption and direct permeation comparable, while the two corresponding P behaviors differ more than 2 orders of magnitude. That can also be observed from the temperature trend of permeability, which decreases at increasing temperature, similar to the solubility coefficient, and opposite to diffusivity.

The mechanism of ammonia permeation in Aquivion membranes, mediated by nano-molecular domains in the ionomer matrix, by means of reversible ammonia-polymer bonding, is also proposed by He and Cussler [18], who characterized ammonia transport in doped Nafion membranes. Furthermore, as other authors [11,25,30] stated, the high NH_3 permeability is due to the formation of ion complex [$-SO_3^- + NH_4^+$] within the matrix which aggregates, causing a phase separation into hydrophobic and hydrophilic domains, which leads to faster transport rate respect to N_2 and H_2.

Considering the experimental evidence, it should be noticed that the Aquivion microstructure modification upon dissolution of ammonia and the interconnectivity of such domains with faster penetrant transport plays a different role during the two types of experiments. In direct permeation tests, indeed, penetrant transport in fast channels, mainly composed of the SO_3^- groups surrounded by ammonia molecules, is predominant; at increasing upstream activity, such regions become highly interconnected, near the percolation limit, thus boosting the NH_3 transport across the membrane.

In transient-sorption tests, on the other hand, due to the intrinsic nature of the experiment (different boundary conditions), the diffusion process targets the dynamics of absorption/dissolution of the gas into polar domains, and the subsequent cluster formation, rather than the flow within them [64,89]. Sorption tests monitor the uptake of ammonia, and they are therefore related to the growth of the dimension and the number of the channels of the percolated structure which do not necessarily follow the same kinetic of the permeation across the membrane.

To conclude the analysis humid gas permeation experiments are also conducted, as the presence of water is known to drastically affect the properties of these materials [90–92], and the electrolytic ammonia production leads to gas mixtures containing water [3].

The change in NH_3 permeability humid conditions (permeability/permeability in dry PFSI) has been plotted as a function of relative humidity in Fig. 7, together with that of other gases already tested in the same materials and the same conditions, in order to compare the effect of moisture on the transport performances of Aquivion of acid, basic or light gases [42,90,93].

Even though ammonia permeability is significantly larger than those of CO_2, N_2, H_2, CH_4, and H_2S, it is also the one that is influenced the least by the presence of water: NH_3 permeability at RH = 80% is 26400 Barrer, only 4 times higher than in that dry condition (5700 Barrer). Conversely, the permeability of the other gases experiences more significant increases: as an example, in the case of acidic gases (e.g., CO_2 and H_2S), permeability increases more than two orders of magnitude, passing from 2.22 to 2 Barrer at RH = 0 to 242 and 370 Barrer at RH = 85%, respectively. Similar behavior is also observed for light gases such as N_2, H_2, or CH_4, which generally show lower increases due to their lower solubility in water. Therefore, the recorded gas permeability increase is mainly related to the formation of water-swollen hydrophilic domains that allow for faster gas transport at increasing relative humidity.

Interestingly, the situation in the case of ammonia is completely different: this gas is already able to swell the membrane and to produce the network of facilitated transport channels, in a similar fashion to water, thus decreasing the effect related to the presence of humidity in the gas stream. From another point of view, the analysis of humid gas permeability suggests the existence of competitive sorption between water and NH_3, which both compete for the same acid $-SO_3H$ sites, so that the water sorbed is lowered by the presence of NH_3. It is indeed well known that water sorption in ammonium-substituted Nafion is lower

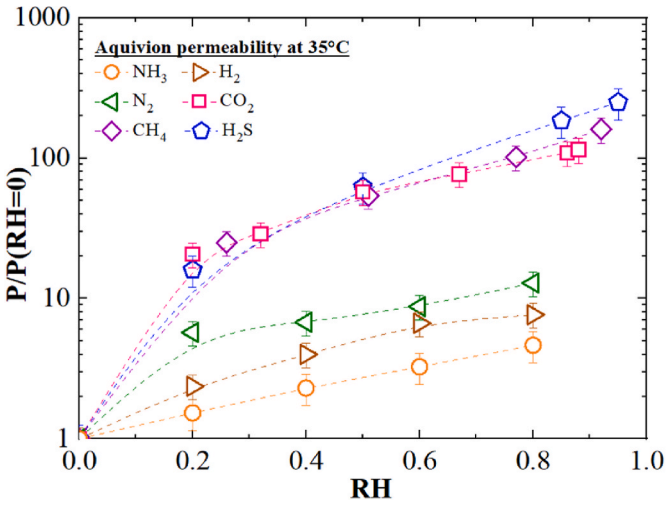

Fig. 7. *Comparison of different gas permeation in humid conditions in Aquivion membranes at atmospheric upstream pressure.*

than in the acidic form, indicating that water molecules are less able to interact with $–SO_3H$ groups when ammonia (or ammonium counterions) is present [18,78,94]. That leads to a reduced effect of relative humidity on ammonia permeability with respect to the other gases inspected [90–92].

Finally, due to the increased attention to green ammonia separation, it is also worthwhile to consider the ideal selectivity for NH_3/N_2 and NH_3/H_2, which can be calculated as the ratio between NH_3 and N_2 and H_2 permeability. The data obtained for Aquivion C87-05 are displayed in the permeability-selectivity plot in Fig. 8 with red dots, compared to the performances of other materials, as obtained from the literature [17,19,25,30,95–98].

Interestingly, the ideal NH_3 perm-selectivity values in Aquivion C87-05 reported in this work are basically the highest ever achieved both with respect to nitrogen and hydrogen. The obtained performances, indeed, are even better than those of similar PFSA materials, at least for pure gas permeation (e.g. Wakimoto et al. [25] who analyzed fluorinated sulfonic acid/ceramic membranes); although competitive sorption and/or swelling phenomena may lead to a reduction of membrane performances. It is shown that NH_3 permeability is at least one order of magnitude lower for the literature data (Nafion, Aquivion, and Aquivion-Li^+/ceramic membranes) with respect to our case, passing from $> 10^2$ Barrer (reported by Wakimoto) to $\approx 10^4$ Barrer (this work, red dots), in spite of the different operative temperature of the tests [25].

Moreover, both NH_3/N_2 and NH_3/H_2 selectivities of Aquivion C87-05 are more than the double than those of similar materials reported in the literature. It is also worth to notice that a slight decrease in selectivity occurs passing from dry to humid conditions (RH = 80%) for both pairs of gases, even though NH_3 permeability rises from 2300 at RH80% to 6690 Barrer in dry conditions. In particular, NH_3/N_2 selectivity is reduced from 9600 to 3120, while NH_3/H_2 selectivity ranges between 1260 and 690 due to the presence of water clusters in the polymer matrix that occupy the $–SO_3H$ groups by decreasing the performance of the membrane.

Fig. 8 includes, as a reference, the upper-bound curve calculated from pure penetrant data, following the approach proposed by Freeman [22], for both gas pairs. The model approach determines the slope of the curve from the kinetic diameter difference (d_k: 260 p.m. for NH_3, 289 p.m. for H_2, and 364 p.m. for N_2), while the position of the curve is mainly related to the relative solubility of the different penetrants, estimated from the Lennard-Jones temperature (ε/K: 558 K for NH_3, 60 K for H_2, and 71 K for N_2). As one can see, a well-defined upper-bound between permeability and selectivity can be determined in the case of NH_3/N_2 separation (black line in Fig. 8a), due to an appreciable difference in the size of the 2 penetrants. Conversely, in the case of NH_3/H_2, the two gases are characterized by a very similar size, and the curve results in an almost flat curve (dotted black line in Fig. 8b), located at quite high selectivity given by the different condensability. In the latter case, indeed, the upper-bound is not really meaningful, as already discussed by Robeson first [23,24], and later analyzed by Freeman [22].

Regarding the NH_3/N_2 selectivity, it is noteworthy that plenty of the experimental data included in the plot are actually overcoming such limits, most of them being PFSA membranes. That has to be ascribed to the peculiar nature of the ammonia/polymer interaction and to the facilitated transport of NH_3 in the membrane.

Finally, the results obtained in this work indicate that, to the best of the authors' knowledge, Aquivion C87-05 is potentially the most indicated material for the targeted separation, with the best perm-selectivity for NH_3/H_2 separation and overall performance far beyond the theoretical upper-bound for NH_3/N_2.

5. Conclusion

Aquivion C87-05 material has been studied as a possible candidate for ammonia gas separation for H_2 and N_2 containing streams to obtain greener energy processes. In this concern, the Aquivion membrane is characterized via transient sorption and steady-state permeation at 20, 35, and 50 °C by using pure ammonia gas, both in dry and humid conditions, and the results are compared with those of hydrogen and nitrogen.

Aquivion C87-05 exhibits extremely high NH_3 solubility even higher than that of water, and with a very limited influence on temperature. The IR analysis shows that NH_3 release is very slow after sorption and suggests that solvation interactions are formed in the materials between ammonia and the sulfonic groups present in the polymer side chains. In particular, the hypothesis of clusters formation including 3 or 4 ammonia molecules per ionic group are needed to obtain a good description of the sorption isotherms through a theoretical model, based on Flory-Huggins and adapted to account for electrostatic polymer-penetrant interactions.

Aquivion C87-05 also exhibits extremely high NH_3 permeability, which, in dry conditions, reaches values around 17000 Barrer at 20 °C, and shows an increasing trend with upstream pressure. All the different experimental evidences indicate that ammonia transport through the membrane is actually driven by solubility rather than by diffusivity within the polymer matrix, even though the strong interaction and the large modification of the polymer upon sorption prevent the use of solution diffusion model. Moreover, these membranes show very high ideal selectivity of ammonia with respect to other gases, with values up to 7000 for the NH_3/N_2 pair and in the order of 1000 for NH_3/H_2.

Compared to other gases, such as CO_2 and H_2S, or even light gases (N_2 or H_2) the presence of water produces a limited effect on the ammonia permeability, as a consequence of the acid-base affinity with the functional groups of the polymers, rather than the molecular size and/or the solubility of the gas in water vapor. Such behavior can be related to the competitive sorption between water and ammonia, which

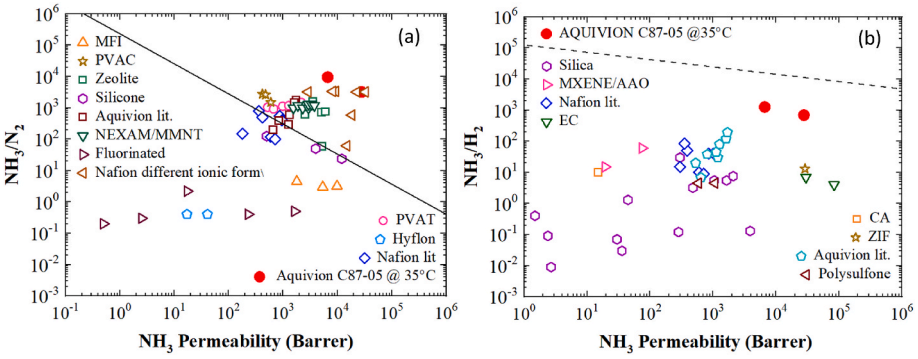

Fig. 8. *Comparison between (a) NH_3/N_2 and (b) NH_3/H_2 Robeson Plot for literature perm-selectivity data in other polymers* [22,25,30,96–100]. *The experimental data obtained in this work are reported with red dots at 35°C for dry and humid conditions (RH80%).* (For interpretation of the references to colour in this figure legend, the reader is referred to the Web version of this article.)

both interact with acidic polymer pendant chains, creating clusters around the sulfonic groups. In addition to that, due to the high solubility, ammonia is expected to form a percolated structure of polar channels within the polymer, which is very similar to that usually formed by water.

Finally, the good separation performances obtained in this work and the intrinsic resistance of Aquivion to harsh environments, suggest that this polymer is an ideal candidate for the separation of hydrogen and nitrogen from NH_3.

CRediT authorship contribution statement

Virginia Signorini: Writing – original draft, Methodology, Investigation, Data curation. **Aysegul Askin:** Writing – review & editing, Methodology, Investigation, Data curation. **Claudio Oldani:** Writing – review & editing, Supervision, Resources. **Matteo Minelli:** Writing – review & editing, Supervision, Data curation. **Marco Giacinti Baschetti:** Writing – review & editing, Supervision, Formal analysis, Data curation, Conceptualization.

Declaration of competing interest

The authors declare the following financial interests/personal relationships which may be considered as potential competing interests: Prof. Marco Giacinti Baschetti reports financial support was provided by European Union. If there are other authors, they declare that they have no known competing financial interests or personal relationships that could have appeared to influence the work reported in this paper.

Data availability

Data will be made available on request.

Acknowledgment

The present work is part of the activities of the Italian Project ECOSISTER funded under the National Recovery and Resilience Plan (NRRP), Mission 04 Component 2 Investment 1.5—NextGenerationEU, Call for tender n. 3277 dated 30 December 2021 Award Number: 0001052 dated 23 June 2022

Prof. A.Askin thanks Diffusion in Polymers and Membrane Separation Research Group of the University of Bologna for providing research opportunities in their laboratories, and the Eskişehir Osmangazi University Scientific Research Projects Commission (GR/202115008) for financial support.

References

[1] L. Zhang, H. Dong, S. Zeng, Z. Hu, S. Hussain, X. Zhang, An overview of ammonia separation by ionic liquids, Ind. Eng. Chem. Res. 60 (2021) 6908–6924, https://doi.org/10.1021/ACS.IECR.1C00780/ASSET/IMAGES/MEDIUM/IE1C00780_0016.GIF.

[2] A. Afif, N. Radenahmad, Q. Cheok, S. Shams, J.H. Kim, A.K. Azad, Ammonia-fed fuel cells: a comprehensive review, Renew. Sustain. Energy Rev. 60 (2016) 822–835, https://doi.org/10.1016/J.RSER.2016.01.120.

[3] B. Wang, T. Li, F. Gong, M.H.D. Othman, R. Xiao, Ammonia as a green energy carrier: electrochemical synthesis and direct ammonia fuel cell - a comprehensive review, Fuel Process. Technol. 235 (2022) 107380, https://doi.org/10.1016/J.FUPROC.2022.107380.

[4] S. Giddey, S.P.S. Badwal, A. Kulkarni, Review of electrochemical ammonia production technologies and materials, Int. J. Hydrogen Energy 38 (2013) 14576–14594, https://doi.org/10.1016/J.IJHYDENE.2013.09.054.

[5] Z. Wan, Y. Tao, J. Shao, Y. Zhang, H. You, Ammonia as an effective hydrogen carrier and a clean fuel for solid oxide fuel cells, Energy Convers. Manag. 228 (2021) 113729, https://doi.org/10.1016/J.ENCONMAN.2020.113729.

[6] K.E. Lamb, M.D. Dolan, D.F. Kennedy, Ammonia for hydrogen storage; A review of catalytic ammonia decomposition and hydrogen separation and purification, Int. J. Hydrogen Energy 44 (2019) 3580–3593, https://doi.org/10.1016/J.IJHYDENE.2018.12.024.

[7] M. Aziz, A. TriWijayanta, A.B.D. Nandiyanto, Ammonia as effective hydrogen storage: a review on production, storage and utilization, 2020, Energies 13 (2020) 3062, https://doi.org/10.3390/EN13123062, 3062 13.

[8] J. Humphreys, R. Lan, S. Tao, Development and recent progress on ammonia synthesis catalysts for haber–bosch process, Advan. Energy Sustain. Res. 2 (2021) 2000043, https://doi.org/10.1002/AESR.202000043.

[9] G. Soloveichik, Electrochemical Synthesis of Ammonia as a Potential Alternative to the Haber–Bosch Process, 1929, https://doi.org/10.1038/s41929-019-0280-0.

[10] M. Malmali, G. Le, J. Hendrickson, J. Prince, A.V. McCormick, E.L. Cussler, Better absorbents for ammonia separation, ACS Sustain. Chem. Eng. 6 (2018) 6536–6546, https://doi.org/10.1021/ACSSUSCHEMENG.7B04684/ASSET/IMAGES/MEDIUM/SC-2017-04684E_0009.GIF.

[11] M. Kanezashi, A. Yamamoto, T. Yoshioka, T. Tsuru, Characteristics of ammonia permeation through porous silica membranes, AIChE J. 56 (2010) 1204–1212, https://doi.org/10.1002/AIC.12059.

[12] E. Ruiz, V.R. Ferro, J. De Riva, D. Moreno, J. Palomar, Evaluation of ionic liquids as absorbents for ammonia absorption refrigeration cycles using COSMO-based process simulations, Appl. Energy 123 (2014) 281–291, https://doi.org/10.1016/J.APENERGY.2014.02.061.

[13] A. Klerke, C.H. Christensen, J.K. Nørskov, T. Vegge, Ammonia for hydrogen storage: challenges and opportunities, J. Mater. Chem. 18 (2008) 2304–2310, https://doi.org/10.1039/B720020J.

[14] J. Zheng, L. Jiang, Y. Lyu, S.P. Jiang, S. Wang, Green synthesis of nitrogen-to-ammonia fixation: past, present, and future, Energy Environ. Mater. 5 (2022) 452–457, https://doi.org/10.1002/EEM2.12192.

[15] J. Turner, G. Sverdrup, M.K. Mann, P.C. Maness, B. Kroposki, M. Ghirardi, R. J. Evans, D. Blake, Renewable hydrogen production, Int. J. Energy Res. 32 (2008) 379–407, https://doi.org/10.1002/ER.1372.

[16] L. Vermaak, H.W.J.P. Neomagus, D.G. Bessarabov, Hydrogen separation and purification from various gas mixtures by means of electrochemical membrane technology in the temperature range 100–160 °C, 2021, Membranes 11 (2021) 282, https://doi.org/10.3390/MEMBRANES11040282, 282 11.

[17] Q. Wei, J.M. Lucero, J.M. Crawford, J.D. Way, C.A. Wolden, M.A. Carreon, Ammonia separation from N2 and H2 over LTA zeolitic imidazolate framework membranes, J. Membr. Sci. 623 (2021) 119078, https://doi.org/10.1016/J.MEMSCI.2021.119078.

[18] Y. He, E.L. Cussler, Ammonia permeabilities of perfluorosulfonic membranes in various ionic forms, J. Membr. Sci. 68 (1992) 43–52, https://doi.org/10.1016/0376-7388(92)80148-D.

[19] D.I. Petukhov, A.S. Kan, A.P. Chumakov, O.V. Konovalov, R.G. Valeev, A. A. Eliseev, MXene-based gas separation membranes with sorption type selectivity, J. Membr. Sci. 621 (2021) 118994, https://doi.org/10.1016/J.MEMSCI.2020.118994.

[20] P. Pandey, R.S. Chauhan, Membranes for gas separation, Prog. Polym. Sci. 26 (2001) 853–893, https://doi.org/10.1016/S0079-6700(01)00009-0.

[21] P. Bernardo, G. Clarizia, 30 years of membrane technology for gas separation, Chem. Eng. Transact. 32 (2013) 1999–2004, https://doi.org/10.3303/CET1332334.

[22] B.D. Freeman, Basis of permeability/selectivity tradeoff relations in polymeric gas separation membranes, Macromolecules (1999).

[23] L.M. Robeson, Polymeric membranes for gas separation, in: Encyclopedia of Materials: Science and Technology, 2001, https://doi.org/10.1016/b0-08-043152-6/01364-4.

[24] L.M. Robeson, The upper bound revisited, J. Membr. Sci. (2008), https://doi.org/10.1016/j.memsci.2008.04.030.

[25] K. Wakimoto, W.W. Yan, N. Moriyama, H. Nagasawa, M. Kanezashi, T. Tsuru, Ammonia permeation of fluorinated sulfonic acid polymer/ceramic composite membranes, J. Membr. Sci. 658 (2022) 120718, https://doi.org/10.1016/J.MEMSCI.2022.120718.

[26] I. Kobayashi, M. Nakajima, K. Chun, Y. Kikuchi, H. Fujita, Silicon array of elongated through-holes for monodisperse emulsion droplets, AIChE J. 48 (2002) 1639–1644, https://doi.org/10.1002/AIC.690480807.

[27] US4761164A - Method for gas separation - Google Patents, (n.d.). https://patents.google.com/patent/US4761164 (accessed June 2, 2023).

[28] D. William, K. Kammermeyer, Separation of Gases by Plastic Membranes PERMEATION RATES AND EXTENT OF SEPARATION, (n.d.). https://pubs.acs.org/sharingguidelines (accessed June 2, 2023)..

[29] S. Kulprathipanja, Mixed matrix membrane development, Membr. Technol. 2002 (2002) 9–12, https://doi.org/10.1016/S0958-2118(02)80132-X.

[30] M.A. Komkova, I.S. Sadilov, V.A. Brotsman, D.I. Petukhov, A.A. Eliseev, Facilitated transport of ammonia in ultra-thin Prussian Blue membranes with potential-tuned selectivity, J. Membr. Sci. 639 (2021) 119714, https://doi.org/10.1016/J.MEMSCI.2021.119714.

[31] S.F. Timashev, A.V. Vorobiev, V.I. Kirichenko, Y.M. Popkov, V.I. Volkov, R. R. Shifrina, A.Y. Lyapunov, A.G. Bondarenko, L.P. Bobrova, Specifics of highly selective ammonia transport through gas-separating membranes based on perfluorinated copolymer in the form of hollow fibers, J. Membr. Sci. 59 (1991) 117–131, https://doi.org/10.1016/S0376-7388(00)81178-3.

[32] M.A. Vandiver, S. Seifert, M.W. Liberatore, A.M. Herring, Synthesis and characterization of perfluoro quaternary ammonium ion exchange membranes for fuel cell applications, ECS Trans. 50 (2013) 2119–2127, https://doi.org/10.1149/05002.2119ECST/XML.

[33] E.Y. Safronova, A.K. Osipov, A.B. Yaroslavtsev, Short side chain aquivion perfluorinated sulfonated proton-conductive membranes: transport and mechanical properties, Petrol. Chem. (2018), https://doi.org/10.1134/S0965544118020044.

[34] V. Arcella, A. Ghielmi, G. Tommasi, High performance perfluoropolymer films and membranes, Ann. N. Y. Acad. Sci. (2003), https://doi.org/10.1111/j.1749-6632.2003.tb06002.x.

[35] G. Gebel, Structural evolution of water swollen perfluorosulfonated ionomers from dry membrane to solution, Polymer (2000), https://doi.org/10.1016/S0032-3861(99)00770-3.

[36] L.M. Costello, W.J. Koros, Temperature dependence of gas sorption and transport properties in polymers: measurement and applications, Ind. Eng. Chem. Res. 31 (1992) 2708–2714, https://doi.org/10.1021/ie00012a012.

[37] J.G. Wijmans, R.W. Baker, The solution-diffusion model: a review, J. Membr. Sci. 107 (1995) 1–21, https://doi.org/10.1016/0376-7388(95)00102-I.

[38] R.W. Baker, Membrane Technology and Applications, 2012, https://doi.org/10.1002/9781118359686.

[39] K. Ghosal, B.D. Freeman, Gas separation using polymer membranes: an overview, Polym. Adv. Technol. (1994), https://doi.org/10.1002/pat.1994.220051102.

[40] E. Ricci, F.M. Benedetti, A. Noto, T.C. Merkel, J. Jin, M.G. De Angelis, Enabling experimental characterization and prediction of ternary mixed-gas sorption in polymers: C2H6/CO2/CH4 in PIM-1, Chem. Eng. J. 426 (2021) 130715, https://doi.org/10.1016/J.CEJ.2021.130715.

[41] J. Crank, The Mathematics of Diffusion, second ed., vol. 1975, Claredon Press - Oxford University Press, 1957, pp. 1267–1268, https://doi.org/10.1021/ja01562a072, 79.

[42] V. Signorini, M. Giacinti Baschetti, D. Pizzi, L. Merlo, Hydrogen sulfide mix gas permeation in Aquivion® perfluorosulfonic acid (PFSA) ionomer membranes for natural gas sweetening, J. Membr. Sci. 640 (2021) 119809, https://doi.org/10.1016/J.MEMSCI.2021.119809.

[43] H.L. Frisch, The Time Lag in Diffusion 93 the TIME LAG IN DIFFUSION*, 1957. https://pubs.acs.org/sharingguidelines. (Accessed 9 June 2023).

[44] S.C. Fraga, M. Monteleone, M. Lanč, E. Esposito, A. Fuoco, L. Giorno, K. Pilnáček, K. Friess, M. Carta, N.B. McKeown, P. Izák, Z. Petrusová, J.G. Crespo, C. Brazinha, J.C. Jansen, A novel time lag method for the analysis of mixed gas diffusion in polymeric membranes by on-line mass spectrometry: method development and validation, J. Membr. Sci. 561 (2018) 39–58, https://doi.org/10.1016/J.MEMSCI.2018.04.029.

[45] H. Wu, J. Thibault, B. Kruczek, The validity of the time-lag method for the characterization of mixed-matrix membranes, J. Membr. Sci. 618 (2021) 118715, https://doi.org/10.1016/J.MEMSCI.2020.118715.

[46] O. Thygesen, M.A.B. Hedegaard, A. Zarebska, C. Beleites, C. Krafft, Membrane fouling from ammonia recovery analyzed by ATR-FTIR imaging, Vib. Spectrosc. 72 (2014) 119–123, https://doi.org/10.1016/J.VIBSPEC.2014.03.004.

[47] U. Riaz, S.M. Ashraf, Characterization of polymer blends with FTIR spectroscopy, Charact. Polymer Blends: Miscibil. Morphol. Interf. 9783527331536 (2015) 625–678, https://doi.org/10.1002/9783527645602.CH20.

[48] Y.A. Elabd, M.G. Baschetti, T.A. Barbari, Time-Resolved fourier transform infrared/attenuated total reflection spectroscopy for the measurement of molecular diffusion in polymers, J. Polym. Sci. B Polym. Phys. 41 (2003) 2794–2807, https://doi.org/10.1002/POLB.10661.

[49] R. Bhargava, S.Q. Wang, J.L. Koenig, FTIR microspectroscopy of polymeric systems, Adv. Polym. Sci. 163 (2003) 137–191, https://doi.org/10.1007/B11052/COVER.

[50] R.H. Lacombe, I.C. Sanchez, Statistical thermodynamics of fluid mixtures, J. Phys. Chem. 80 (1976) 2568–2580, https://doi.org/10.1021/j100564a009.

[51] D.T. Hallinan, M.G. De Angelis, M.G. Baschetti, G.C. Sarti, Y.A. Elabd, Non-Fickian Diffusion of Water in Nafion, 43 (n.d.) 4667. https://doi.org/10.1021/ma100047z..

[52] M. Laporta, M. Pegoraroa, L. Zanderighi, Perfluorosulfonated Membrane (Nafion) : FT-IR Study of the State of Water with Increasing Humidity, (n.d.)..

[53] M.C. Ferrari, J. Catalano, M.G. Baschetti, M.G. De Angelis, G.C. Sarti, FTIR-ATR study of water distribution in a short-side-chain PFSI membrane, Macromolecules (2012), https://doi.org/10.1021/ma202099p.

[54] R. Buzzoni, S. Bordiga, G. Ricchiardi, G. Spoto, A. Zecchina, Interaction of H2O, CH3OH, (CI˙O, CH3CN, and pyridine with the superacid perfluorosulfonic membrane nafion: an IR and Raman study, J. Phys. Chem. 99 (1995) 11937–11951. https://pubs.acs.org/sharingguidelines. (Accessed 28 April 2023).

[55] S. Süzer, L. Andrews, S. Sjze, View Online – Export Citation CrossMark FTIR spectra of ammonia clusters in noble gas matrices FTIR spectra of ammonia clusters in noble gas matrices, J. Chem. Phys. 87 (1987) 5131–5140, https://doi.org/10.1063/1.453681.

[56] E.K. R Echterhoff, FTIR spectroscopic characterization of the adsorption and desorption of ammonia on MgO surfaces, Surf. Sci. 230 (1–3) (1990) 237–244, https://doi.org/10.1016/0039-6028(90)90031-3, 237–244. (Accessed 28 April 2023).

[57] S. Süzer, L. Andrews, FTIR spectra of ammonia clusters in noble gas matrices, J. Chem. Phys. 87 (1987) 5131–5140, https://doi.org/10.1063/1.453681.

[58] M.N. Slipchenko, A.F. Vilesov, Spectra of NH3 in He droplets in the 3 μm range, Chem. Phys. Lett. 412 (2005) 176–183, https://doi.org/10.1016/J.CPLETT.2005.06.100.

[59] M.N. Slipchenko, B.G. Sartakov, A.F. Vilesov, Evolution of the vibrational spectrum of ammonia from single molecule to bulk, J. Chem. Phys. 128 (2008) 134509, https://doi.org/10.1063/1.2884927.

[60] M.N. Slipchenko, B.G. Sartakov, A.F. Vilesov, S.S. Xantheas, Study of NH Stretching Vibrations in Small Ammonia Clusters by Infrared Spectroscopy in He Droplets and Ab Initio Calculations, 2007, https://doi.org/10.1021/JP071279.

[61] A. Malloum, J. Conradie, Hydrogen bond networks of ammonia clusters: what we know and what we don't know, J. Mol. Liq. 336 (2021) 116199, https://doi.org/10.1016/J.MOLLIQ.2021.116199.

[62] D.W. Green, M.Z. Southard Dr., Perry's Chemical Engineers' Handbook, McGraw-Hill Education, 2019. https://www.accessengineeringlibrary.com/content/book/9780071834087. (Accessed 25 April 2023).

[63] M.G. De Angelis, S. Lodge, M. Giacinti Baschetti, G.C. Sarti, F. Doghieri, A. Sanguineti, P. Fossati, Water sorption and diffusion in a short-side-chain perfluorosulfonic acid ionomer membrane for PEMFCS: effect of temperature and pre-treatment, Desalination (2006), https://doi.org/10.1016/j.desal.2005.06.070.

[64] A. Kusoglu, A.Z. Weber, New Insights into Perfluorinated Sulfonic-Acid Ionomers, Chem Rev, 2017, https://doi.org/10.1021/acs.chemrev.6b00159.

[65] W.Y. Hsu, T.D. Gierke, Ion transport and clustering in nafion perfluorinated membranes, J. Membr. Sci. (1983), https://doi.org/10.1016/S0376-7388(00)81563-X.

[66] G. Gebel, J. Lambard, Small-angle scattering study of water-swollen perfluorinated ionomer membranes, Macromolecules (1997), https://doi.org/10.1021/ma970801v.

[67] J. Catalano, M.G. Baschetti, M.G. De Angelis, G.C. Sarti, A. Sanguineti, P. Fossati, Gas and water vapor permeation in a short-side-chain PFSI membrane, Desalination 240 (2009) 341–346, https://doi.org/10.1016/J.DESAL.2007.12.044.

[68] Q. Zhao, P. Majsztrik, J. Benziger, Diffusion and interfacial transport of water in Nafion, J. Phys. Chem. B 115 (2011) 2717–2727, https://doi.org/10.1021/jp1112125.

[69] H.R. Zelsmann, M. Pineri, M. Thomas, M. Escoubes, Water self-diffusion coefficient determination in an ion exchange membrane by optical measurement, J. Appl. Polym. Sci. 41 (1990) 1673–1684, https://doi.org/10.1002/APP.1990.070410726.

[70] D.T. Hallinan, Y.A. Elabd, Diffusion of water in nafion using time-resolved fourier transform infrared-attenuated total reflectance spectroscopy, J. Phys. Chem. B 113 (2009) 4257–4266, https://doi.org/10.1021/JP811325V.

[71] D.R. Morris, X. Sun, Water-sorption and transport properties of Nafion 117 H, J. Appl. Polym. Sci. 50 (1993) 1445–1452, https://doi.org/10.1002/APP.1993.070500816.

[72] M. Legras, Y. Hirata, Q.T. Nguyen, D. Langevin, M. Métayer, Sorption and diffusion behaviors of water in Nation 117 membranes with different counter ions, Desalination 147 (2002) 351–357, https://doi.org/10.1016/S0011-9164(02)00608-2.

[73] Q. Zhao, P. Majsztrik, J. Benziger, Diffusion and interfacial transport of water in Nafion, J. Phys. Chem. B 115 (2011) 2717–2727, https://doi.org/10.1021/JP1112125/SUPPL_FILE/JP1112125_SI_006.PDF.

[74] A.T. Larson, R.L. Dodge, The ammonia equilibrium, J. Am. Chem. Soc. 45 (1923) 2918–2930, https://doi.org/10.1021/JA01665A017.

[75] P. Futerko, I. Hsing, Thermodynamics of water vapor uptake in perfluorosulfonic acid membranes, J. Electrochem. Soc. 146 (1999) 2049–2053, https://doi.org/10.1149/1.1391890/XML.

[76] P.J. Carvalho, J.A.P. Coutinho, Non-ideality of solutions of NH3, SO2, and H 2S in ionic liquids and the prediction of their solubilities using the flory-huggins model, Energy Fuel. 24 (2010) 6662–6666, https://doi.org/10.1021/EF100988Z.

[77] K. Hongsirikarn, J.G. Goodwin, S. Greenway, S. Creager, Influence of ammonia on the conductivity of Nafion membranes, J. Power Sources 195 (2010) 30–38, https://doi.org/10.1016/J.JPOWSOUR.2009.07.013.

[78] A. Bhown, E.L. Cussler, Mechanism for selective ammonia transport through poly (vinylammonium thiocyanate) membranes, J. Am. Chem. Soc. 113 (1991) 742–749. https://pubs.acs.org/sharingguidelines. (Accessed 18 August 2023).

[79] A. Malloum, J. Jules Fifen, J. Conradie, J. Chem Phys, Structures and infrared spectroscopy of large sized protonated ammonia clusters – Articles You May Be Interested in Exploration of the potential energy surface of the ethanol hexamer Structures and spectroscopy of the ammonia eicosamer, (NH 3) n=20 Test case prioritization based on MCCM complexity for event sequence test cases Structures and infrared spectroscopy of large sized protonated ammonia clusters, J. Chem. Phys. 149 (2018) 244301, https://doi.org/10.1063/1.5053172.

[80] K. Hirao, T. Fujikawa, H. Konishi, S. Yamabe, A Theoretical study of ammonia polymers and cluster ions, Chem. Phys. Lett. 104 (1984) 184–190, https://doi.org/10.1016/0009-2614(84)80193-1.

[81] T.A. Beu, U. Buck, Vibrational spectra of ammonia clusters from n=3 to 18, J. Chem. Phys. 114 (2001) 7853–7858, https://doi.org/10.1063/1.1365097.

[82] A. Pullman, A.M. Armbruster, Ab initio investigation of the energy and electronic evolution upon progressive solvation of ammonium ions, Chem. Phys. Lett. 36 (1975) 558–563, https://doi.org/10.1016/0009-2614(75)85337-1.

[83] K.D. Froyd, E.R. Lovejoy, Bond energies and structures of ammonia-sulfuric acid positive cluster ions, J. Phys. Chem. A 116 (2012) 5886–5899, https://doi.org/10.1021/JP209908F.

[84] H. Shinohara, N. Nishi, N. Washida, Photoionization of ammonia clusters: detection and distribution of unprotonated cluster ions (NH 3) + n , n=2-25, J. Chem. Phys. 83 (1985) 1939–1947, https://doi.org/10.1063/1.449331.

[85] S.A. Kulkarni, R.K. Pathak, Ab initio investigations on neutral clusters of ammonia: (NH3)n (n=2–6), Chem. Phys. Lett. 336 (2001) 278–283, https://doi.org/10.1016/S0009-2614(01)00107-5.

[86] Y. Yampolskii, I. Pinnau, B.D. Freeman, Materials Science of Membranes for Gas and Vapor Separation, Materials Science of Membranes for Gas and Vapor Separation, 2006, pp. 1–445, https://doi.org/10.1002/047002903X.

[87] M. Mukaddam, E. Litwiller, I. Pinnau, Gas sorption, diffusion, and permeation in nafion, Macromolecules (2016), https://doi.org/10.1021/acs.macromol.5b02578.

[88] P.W. Majsztrik, M.B. Satterfield, A.B. Bocarsly, J.B. Benziger, Water sorption, desorption and transport in Nafion membranes, J. Membr. Sci. 301 (2007) 93–106, https://doi.org/10.1016/J.MEMSCI.2007.06.022.
[89] M. Giacinti Baschetti, F. Doghieri, B. Freeman, G.C. Sarti, Transient and steady-state effective diffusivity in high free volume glassy polymers, J. Membr. Sci. 344 (2009) 144–154, https://doi.org/10.1016/J.MEMSCI.2009.07.045.
[90] L. Olivieri, H. Aboukeila, M. Giacinti Baschetti, D. Pizzi, L. Merlo, G.C. Sarti, Humid permeation of CO2 and hydrocarbons in Aquivion® perfluorosulfonic acid ionomer membranes, experimental and modeling, J. Membr. Sci. (2017), https://doi.org/10.1016/j.memsci.2017.08.030.
[91] M. Giacinti Baschetti, M. Minelli, J. Catalano, G.C. Sarti, Gas permeation in perflurosulfonated membranes: influence of temperature and relative humidity, Int. J. Hydrogen Energy (2013), https://doi.org/10.1016/j.ijhydene.2013.06.104.
[92] J. Catalano, T. Myezwa, M.G. De Angelis, M.G. Baschetti, G.C. Sarti, The effect of relative humidity on the gas permeability and swelling in PFSI membranes, Int. J. Hydrogen Energy 37 (2012) 6308–6316, https://doi.org/10.1016/J.IJHYDENE.2011.07.047.
[93] L. Olivieri, R. Trichkov, D. Pizzi, L. Merlo, M.G. Baschetti, The effect of pressure and mixed gas composition on humid CO2 and hydrocarbons permeation in Aquivion® PFSA, J. Membr. Sci. (2018), https://doi.org/10.1016/j.memsci.2018.08.048.
[94] A.P. Abbott, G. Capper, D.L. Davies, H.L. Munro, R.K. Rasheed, V. Tambyrajah, Preparation of novel, moisture-stable, lewis-acidic ionic liquids containing quaternary ammonium salts with functional side chains, Chem. Commun. 1 (2001) 2010–2011, https://doi.org/10.1039/b106357j.
[95] B. Yang, L. Bai, T. Li, L. Deng, L. Liu, S. Zeng, J. Han, X. Zhang, Super selective ammonia separation through multiple-site interaction with ionic liquid-based hybrid membranes, J. Membr. Sci. 628 (2021) 119264, https://doi.org/10.1016/J.MEMSCI.2021.119264.
[96] C. Makhloufi, D. Roizard, E. Favre, Reverse Selective NH 3/CO 2 Permeation in Fluorinated Polymers Using Membrane Gas Separation, 2013, https://doi.org/10.1016/j.memsci.2013.03.048.
[97] B. Yang, L. Bai, S. Zeng, S. Luo, L. Liu, J. Han, Y. Nie, X. Zhang, S. Zhang, NH 3 separation membranes with self-assembled gas highways induced by protic ionic liquids, Chem. Eng. J. 421 (2021) 127876, https://doi.org/10.1016/j.cej.2020.127876.
[98] I.V. Vorotyntsev, P.N. Drozdov, N.V. Karyakin, Ammonia permeability of a cellulose acetate membrane, Inorg. Mater. 42 (2006) 231–235, https://doi.org/10.1134/S0020168506030034/METRICS.
[99] V. Daniel, L. Laciak, R. Quinn, G.P. Pez, J.B. Appleby, P.S. Puri, Selective permeation of ammonia and carbon dioxide by novel membranes, Separ. Sci. Technol. 25 (1990) 1295–1305, https://doi.org/10.1080/01496399008050392.
[100] S.A. Stern, B.D. Bhide, Permeability of silicone polymers to ammonia and hydrogen sulfide, J. Appl. Polym. Sci. 38 (1989) 2131–2147, https://doi.org/10.1002/APP.1989.070381114.